Solid State Science and Technology, Vol. 17, No 2 (2009) 82-88
ISSN 0128-7389

MAGNETORESISTIVE AND MAGNETIC PROPERTIES OF $La_{0.67}A_{0.33}MnO_3$ (A= Ba, Ca, and Sr) PREPARED BY CO-PRECIPITATION METHOD

S. W. Ng, K. P. Lim, S. A. Halim, S. K. Chen and J. K. Wong

Physics Department, Faculty of Science, Universiti Putra Malaysia, 43400 UPM Serdang, Selangor, Malaysia

ABSTRACT

We have prepared perovskite structured $La_{0.67}A_{0.33}MnO_3$ manganite (A = Ba, Ca and Sr) using co-precipitation method. The samples were characterized using x-ray diffraction (XRD) and scanning electron microscope (SEM) to identify the structure and microstructure. The magnetic and magnetoresistance properties were measured by vibrations sample magnetometer (VSM) and four point probe methods. From the XRD spectrum, samples are in single phase pervoskite structure where LBMO and LCMO showed orthorhombic whereas LSMO has rhombohedral phase. LSMO has average grain size range of 0.5μm -2.5μm. However, for LBMO and LCMO, the grain boundaries are not well define and connected. The difference in the microstructure image might be due to the different activation energy and variance A-site cation that differs in grain growth. The Curie temperature of LBMO and LSMO are 343K and 371K, respectively. LCMO system gives the highest CMR value (-10.1% at 1 tesla) at room temperature. A significantly low field magnetoresistance effect (LFMR) which is -13.9% (at 0.1T, 90K) has been observed in LBMO and this LFMR effect is believed to be due to the disorder layers at the grain boundaries in the samples.

INTRODUCTION

Perovskite manganite $La_{1-x}A_xMnO_3$ (A = Ca, Ba, and Sr) are useful for various industrial applications and attracted a considerable attention due to its colossal magnetoresistance (CMR) behavior with a magnetic resistance ratio of more than 100% around the Curie temperature (T_c) [1]. CMR ratio is defined as $(\rho_0-\rho_H)/\rho_0$, where ρ_0 and ρ_H are the resistivities measured at zero and H field. However, large magnetic field of the order of several teslas required to obtain significant effect. For most room temperature applications one needs a significant MR at lower magnetic field [2]. The parent $LaMnO_3$ compound is A-type anti-ferromagnetic insulator with a small ferromagnetic component due to the non-collinearity of the manganese magnetic moments, i.e., weak ferromagnetic. By substitution of La^{3+} with the divalent cation (A^{2+}), La-A-Mn-O can be driven into an electrical and magnetic phase transition [3]. The basic for the theoretical explanation of the perovskite manganese oxides is usually the notion of double exchange interaction (DE) by Zener [4-5]. The DE interaction is a phenomenon of electron hopping between oxygen coupled Mn^{3+} and Mn^{4+} ions that attribute the conduction. The charge transportation is favored when the spin of Mn ions are parallel to each other. However, DE alone could not explain the experimental data. It has been claimed that an additional mechanism, Jahn-Teller distortion could be

Corresponding Author: weisiau14@yahoo.co.uk

responsible for the transport properties. The Jahn-Teller effects causes further splitting degeneracy d e_g of Mn^{3+} in MnO_6 octahedral. These properties are strongly influenced by the size of cation (A^{2+}) substituted into La-site. It is believed that, the variance of A-site cation radii control the magnetic and electrical properties of perovskite manganites hence influences the values of T_c[6]. Therefore, an effort has been made to correlate the anomalous variation of T_c and MR observed among the samples of the recent investigation with varying ionic radii of A-site cation.

METHODOLOGY

Polycrystalline samples with compositional formula, $La_{0.67}A_{0.33}MnO_3$ (A= Ca, Ba and Sr) were prepared by co-precipitation methods. The stoichiometric proportion of lanthanum (III) Acetate (99.99%), calcium acetate hydrate (97%), strontium acetate hemihydrate (99.9%), barium acetate (99.0%) and manganese (II) acetate tetrahydrate (99+ %) were mixed and resolved in acetic acid to form an aqueous solution containing two or more metal ions. A chemical reaction resulting the drying formation of precipitation. After drying, the precipitated powders (light pink colour) were calcined in furnace at 800˚C for 12 hours, reground, pressed into pellets and sintered in furnace at 1200^{o}C for 24 hours. All the samples were characterized by X-ray diffraction (XRD, PHILIPS) using a Cu Kα radiation in the range of 20-80^o. Scanning electron microscope (SEM, LEO1455 VPSEM) were carried out to investigate the surface morphology. The magnetic transition temperatures (Tc) were obtained from 308K to 373K using Vibration Sample Magnetometer (VSM, Lake Shore 7400). A four-point probe system, which is inserted in the liquid nitrogen cryostat, was used to measure the change in resistance under an external applied magnetic field up to 1 tesla with the measured temperature ranging from 90K to 300K.

RESULT AND DISCUSSION

It is found that the XRD pattern before and after sintering have some difference as shown in Figure 1. Before sintering, the XRD spectrum showed mix phases where the manganites pervoskite and starting precursor powder peaks (as showed as *) are observed, indicated that part of the powder have been reacted during calcination process (800^{o}C, 12 hours). After sintering for 24 hours at 1200^{o}C, those extra peaks are missing due to the complete reaction of the precipitated powders to form manganites phase in the LBMO, LCMO and LSMO systems. Comparing to the standard ICDD (references code 01-089-0569, 00-050-0308 and 00-049-0416 for $La_{0.67}Ba_{0.33}MnO_3$ (LBMO), $La_{0.67}Ca_{0.33}MnO_3$ (LCMO) and $La_{0.67}Sr_{0.33}MnO_3$ (LSMO) respectively), the bulk samples have completely formed into a single phase compound. LBMO and LCMO showed orthorhombic system whereas LSMO showed rhombohedral system. The sintering temperature is lower than that required for conventional solid-state reaction of oxide powders. This might be due to the co-precipitation technique produce smaller and more homogenous powder as compare to conventional solid-state reaction method [7.9].

Corresponding Author: weisiau14@yahoo.co.uk

Solid State Science and Technology, Vol. 17, No 2 (2009) 82-88
ISSN 0128-7389

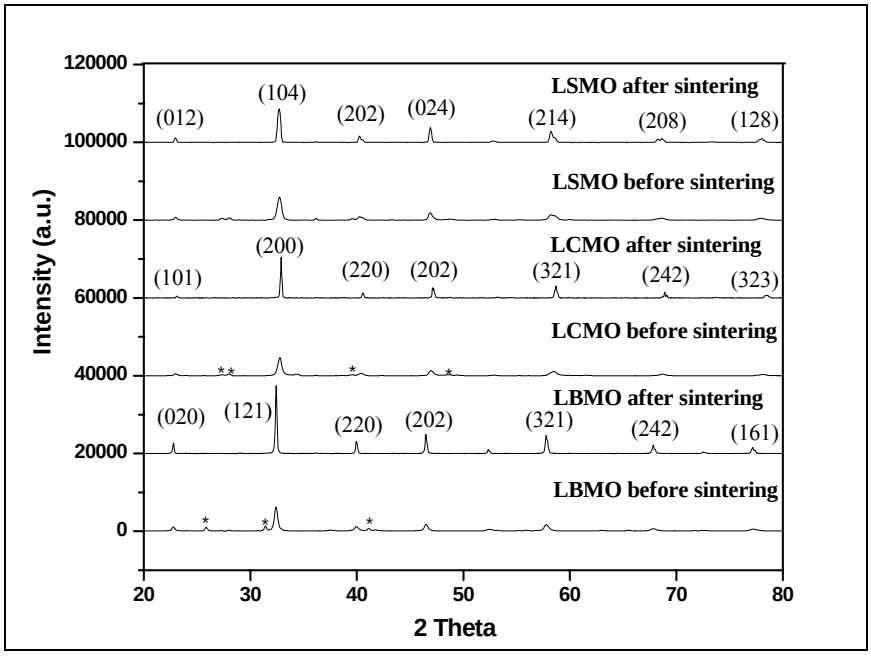

Figure 1: XRD diffraction pattern before and after sintering for LBMO, LCMO and LSMO

Figure 2 shows the scanning electron microscope images of the samples. Scanning electron micrograph showed that LBMO has the smallest average grain size (0.5μm - 2.5μm) as compared to that of LCMO and LSMO systems. This might be due to the atomic radius of Ba is bigger and the activation energy of Ba is higher than Ca and Sr, thus, Ba atom reacts slowly as compare to Ca and Sr [6]. There are no clear grain boundary that can be observed in LCMO and LSMO where all the grains are well connected. More pores are observed in LSMO sample. This indicated that LCMO is more compact as compare to LSMO. The difference in the microstructure images might be due to the variance of A-site cation that differs in grain growth.

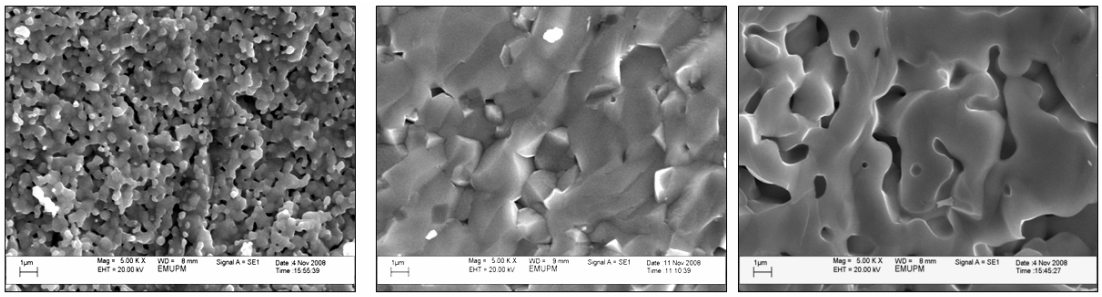

$La_{0.67}Ba_{0.33}MnO_3$ $La_{0.67}Ca_{0.33}MnO_3$ $La_{0.67}Sr_{0.33}MnO_3$

Figure 2: SEM micrographs of the surface of LBMO, LCMO and LSMO

Corresponding Author: weisiau14@yahoo.co.uk

Solid State Science and Technology, Vol. 17, No 2 (2009) 82-88
ISSN 0128-7389

The change in resistance under external applied magnetic field at 1 Tesla from 90K to 300K are as shown in Figure 3. The results show that, at all temperature, the resistivity is found to decrease with the increasing of magnetic field. When an external field is applied, the orientations of the localized spins in samples align parallel with each others. Thus, the Double-Exchange mechanism between Mn^{3+}-O-Mn^{4+} is enhanced and the conductivity increases. All samples did not saturate over the range of 1 Tesla, indicating that the higher magnetic field is needed to align all the spins. All the samples show two obvious regions of MR% slope with different gradients. A sudden drop of magnetoresistance in low magnetic field region (0-0.2T) are -13.9% (at 0.1T, 90K), -8.6% (at 0.2T, 90K) and -10.4% (at 0.2T, 90K) for LBMO, LCMO and LSMO, respectively. This is then followed by an almost linear and slower slops in higher magnetic field (>0.2T). The initial drop of MR is known as low-field magnetoresistance effect (LFMR) where the spin-dependent tunneling and scattering at the interfaces of the grain boundaries are believed to be responsible for this effect [10]. LCMO show relatively small or can be neglected LFMR effect. This could be due to the microstructure form in this sample. From the SEM, no clear grain or grain boundary is observed from the LCMO sample. Therefore, spin dependent tunneling and scattering effect is not significantly taking place.

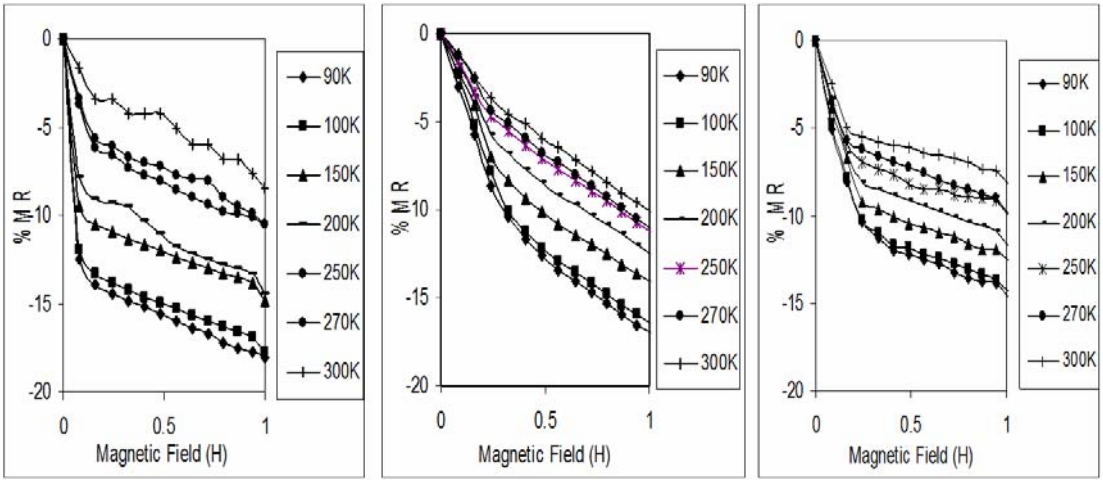

Figure 3: %MR curves of LBMO, LCMO and LSMO at 1 Tesla

The highest CMR value was found in LBMO system (-18.1%) followed by LCMO system (-17.7 %) and LSMO system (-14.5%) at 90K under 1 Tesla field as showed in Figure 4. However, LCMO showed highest CMR value at room temperature which is -10.1% at 1 Tesla. The MR% slope shows magnetoresistance effects over a whole temperature range. This observation is typical for polycrystalline compound where the highest MR value is not observed near T_p and T_c, but increases with the drop of temperature [11].

Corresponding Author: weisiau14@yahoo.co.uk

Solid State Science and Technology, Vol. 17, No 2 (2009) 82-88
ISSN 0128-7389

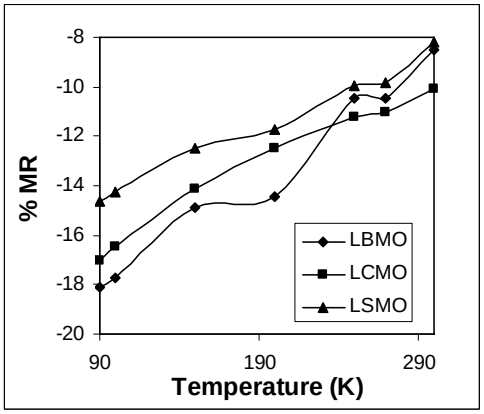

Figure 4: %MR curves of LBMO, LCMO and LSMO at various temperatures at 1 tesla

Figure 5 shows the derivative of magnetization (dm/dT) against temperature from 313K to 373K. From the previous study, T_c for LCMO samples is 224K which is smaller then the measurement range [12]. The measured Curie temperature of LBMO and LSMO systems are 343K and 371K, respectively. This result is slightly higher than the reported value [13]. The insert of Figure 5 showed that LSMO have higher saturated magnetization values as compared to LBMO. It is know that, LBMO having smaller grain size and caused magnetically disordered states in the surface of grain increases. By decreasing the grain size these magnetically disordered states increases and therefore double exchange (DE) mechanism weakens [14].

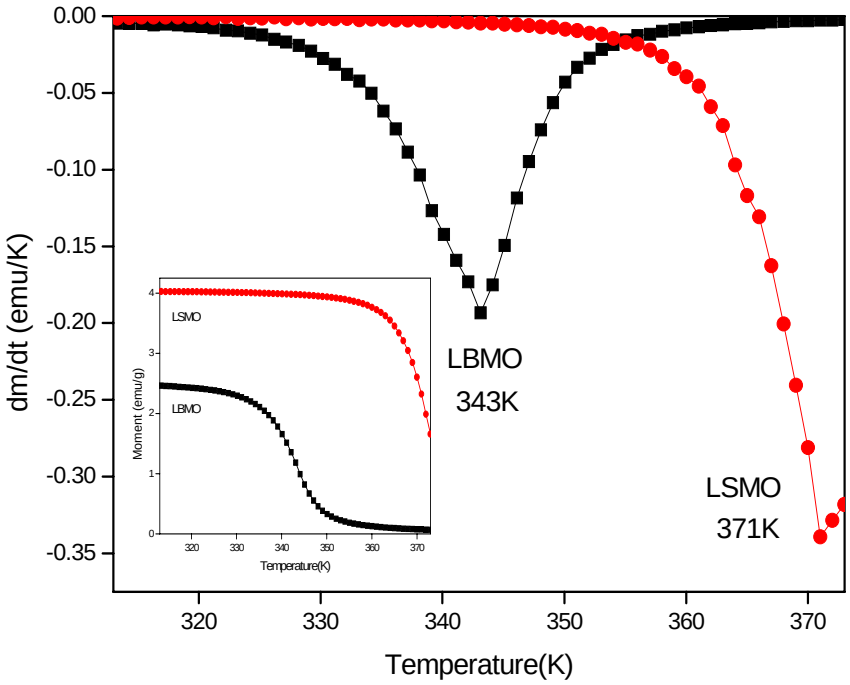

Figure 5: The dm/dT vs. temperature curve for LBMO and LSMO. Inset: Magnetization (emu/g) vs. temperature curve

Corresponding Author: weisiau14@yahoo.co.uk

CONCLUSION

In this work, $La_{0.67}A_{0.33}MnO_3$ (A = Ca, Ba and Sr) have been successfully prepared via co-precipitation method. XRD results showed that single phase compound had been synthesized where LBMO and LCMO showed orthorhombic phase while LSMO the showed rhombohedral phase. LBMO has smallest grain size distribution, however for LCMO and LSMO the grains are well connected with no clear grain boundary. This marked difference of the surface morphology might be due to the different activation energy and variation of A-site cation radius. The Curie temperatures of LBMO and LSMO systems were 343K and 371K, respectively. From the MR measurement, the highest CMR was found in LBMO system (-18.1%) followed by LCMO system (-17.7 %) and LSMO system (-14.5%) at 90K. LBMO showed significant low field magnetoresistance effect which is -13.9% (at 0.1T, 90K) due to the grain boundaries effect that have different magnetization value.

ACKNOWLEDGEMENTS

The Ministry of science, technology and Innovation of Malaysia is gratefully acknowledged for the grant under Science Fund vote: 03-01-04-SF0088: Fabrication of Multilayers Manganite Thin Film having LFMR Effect Using Pulsed Laser Ablation Technique.

REFERENCES

[1]. Y. Tokura, A. Urushibara, Y. Moritomi, T. Arima, A. Asamitsu, G. Kido, N. Furukawa, (1994), *J. Phys. Soc. Jpn,* **63** 3931
[2]. J.S. Moodera, L.R. Kinder, T.M. Wong, R. Meservey, (1995), *Phys. Rev. Lett*. **74** 3273
[3]. B. M. Nagabhushana, R. P. Sreekanth Chakradhar, K. P. Ramesh, C. Shivakumara, G.T. Chandrappa, (2006), *Materials Reasearch Bulletin* **41** 1735-1746
[4]. C. Zener, (1951), *Phys. Rev* **82** 403
[5]. S.L. Young, Y.C. Chen, Lance Horng, T.C. Wu, H.Z. Chen, J.B. Shi, (2000), *Journal of Magnetism Magnetic Material* **289** 145-147
[6]. H.S. Im, G.B. Chon, Sang M. Lee, B.H. Koo, C.G. Lee, M.H. Jung, (2007), *Journal of Magnetism and Magnetic Material* **310** 2668-2670
[7]. Y.B. Zhang, S. Li, C.Q. Sun, T. Sritharan, (2006), *Solid State Communications* **139** 506–510
[8]. Jifan Hu, Hongwei Qin, Hongdong Niu, Luming Zhu, Juan Chen, Weiwei Xiao, Yu Pei, (2003), *Journal of Magnetism and Magnetic Materials* **261** 105–111
[9]. Shahnaz Beguma, Yasuhiro Onoa, Hiroyuki Fujishirob, Tsuyoshi Kajitania, (2006), *Physica B* **385–386** 53–56
[10]. L.F. Zhao, W. Chen, J.L. Shang, Y.Q. Wang, G.O. Yu, X. Xiao, J.F. Miao, Z.C. Xia, S.L. Yuan, (2006) *Materials Science and Engineering B* **127**, 193-197
[11]. K. Frohlich,, I. Vavra, F. Gomory, J. Souc, J. Bydzovsky, P. Kovac, J.

Corresponding Author: weisiau14@yahoo.co.uk

Dobrovodsky, M. Marysko, (2000), *Journal of Magnetism and Magnetic Materials* **211** 67-72
[12]. Pankaj Srivastava, O.N. Srivastava, H.K. Singh, P.K. Siwach, doi:10.1016/j.jallcom.2007.05.033
[13]. G. Venkataiah, V. Prased, P. Venugopal Reddy, *Journal of Alloy and Compounds* 429 (2007) 1-9.
[14]. P. Kameli , H. Salamati, A. Aezami, *J. Alloys Comp.* (2006), doi: 10.1016/j.Jallcom.2006.10.078

Corresponding Author: weisiau14@yahoo.co.uk